WATER RESOURCES RESEARCH, VOL. 33, NO. 12, PAGES 2865–2880, DECEMBER 1997

Stochastic forcing of sediment routing and storage in channel networks

Lee Benda
Earth Systems Institute, Seattle, Washington

Thomas Dunne
School of Environmental Science and Management, University of California, Santa Barbara

Abstract. The stochastic field of sediment supply to the channel network of a drainage basin depends on the large-scale interactions among climatically driven processes such as forest fire and rainstorms, topography, channel network topology, and basin scale. During infrequent periods of intense erosion, large volumes of colluvium are concentrated in parts of a channel network, particularly near tributary junctions. The rivers carry bed material and wash load downstream from these storage sites at different rates. The bed material travels slowly, creating transient patterns of sediment transport, sediment storage, and channel morphology along the channel network. As the concentrations of bed material migrate along the network their waveforms can undergo changes by diffusion, interference at tributary junctions, and loss of mass through temporary sediment storage in fans and terraces and through particle abrasion, which converts bed material to wash load. We investigated how these processes might influence the sediment mass balance in channels of third and higher order in a 215-km^2 drainage basin within the Oregon Coast Range over a simulated 3000-year period with a climate typical of the late Holocene. We used field measurements and a simulation model to illustrate interactions between the major controls on large-scale processes functioning over long periods of time in complex drainage basins.

1. Introduction

The discrete nature of hillslope erosion, in both space and time, creates a strong stochastic influence on the sediment supply to channel networks. However, the resulting sediment supply regime varies systematically with drainage basin size when averaged over long periods of time, and it is possible to analyze how various process controls (climatic, topographic, and geotechnical) affect the stochastic sediment regime [*Benda and Dunne*, this issue]. The stochastic field of sediment supply generates pulses of suspended and bed load transport and of bed-material storage in a channel network. *Nicholas et al*. [1995] use the term "slugs" for these bed-material features and present a classification of them. We use the term "wave" because it is already employed in the literature for such features and seems to be clearly understood there [*Gilbert*, 1917; *Griffiths*, 1979; *Meade*, 1985; *Madej and Ozaki*, 1996]. We do not imply that all of the sediment moves as coherent waves (although the examples above suggest that this is widespread) or that the waves are regular in either form or behavior. They may range in size from a single gravel bar to several-kilometer-long reaches of valley floor that become inundated with sediment moving through a series of almost stationary point bars. They may even be scoured rapidly through canyon reaches with only patches of sediment in storage. We use the terminology of waves to indicate only that there exist in the channel network unsteady and nonuniform variations of transport and storage volumes that may travel or remain stationary and that they can be usefully characterized with a Fourier transform or wavelet transform, like other geophysical signals.

Paper number 97WR02387.
0043-1397/97/97WR-02387$09.00

The waves of sediment eroded from hillslopes enter a channel network that is convergent and hierarchical [*Horton*, 1945]. As the waves travel along this network, four transformations of them may occur: (1) translation, (2) diffusion, (3) mutual interference at tributary junctions, and (4) change of mass through attrition of bed-material particles to wash load or through exchanges with deposits in the valley floor. The original signal of sediment supply that systematically reflects the topographic, geotechnical, and climatic properties and scale of the drainage basin [*Benda and Dunne*, this issue] is gradually transformed along the network, while retaining a strong stochastic influence on the sediment transport and storage in any reach of the channel network.

We illustrate this general principle with a conceptual and simulation model of sediment transport and storage in the channel network of a particular landscape, the central Oregon Coast Range [*Benda and Dunne*, this issue, Figure 1], where the sediment is supplied dominantly by mass wasting, and bed material travels mainly as gravelly bedload. We also use circumstantial field evidence to indicate that the unsteady sediment supply affects channel morphology in the Oregon Coast Range, as others have concluded elsewhere (*Pain and Hosking* [1970], *Griffiths* [1979], *Beschta* [1984], and *Pearce* [1986] in New Zealand; *Ouchi* [1987] in Japan; *Klock and Helvey* [1976], *Swanson and Lienkaemper* [1978], *Lisle* [1982], and *Madej* [1982] in the northwestern United States; and *Wohl and Pearthree* [1991] in the southwestern United States).

Instead of viewing these highly variable aspects of sediment supply and transport as unpredictable, however, we examine

those features of the sediment regime about which generalizations can be made. Although it may be difficult to predict the specific condition of a dynamic sediment transporting system, it is possible to compute the probability of its being in various states as a result of a combination of environmental controls and thus to characterize the sediment regime of any channel reach in terms of its statistical properties. After first explaining how such waves of sediment arise in the particular circumstances of the central Oregon Coast Range, and how they might be simulated with a relatively simple process-based model, we illustrate how characteristic frequencies, magnitudes, and spatial distributions of wave-like sediment transport reflect the climatic regime, basin topography, network topology, and prior movement history of the waves.

The present application requires a considerable amount of empirical data, which in principle could be replaced with more detailed theoretical representations of transport, though such a step would require both theoretical advances and a greater investment in parameter evaluation. Here, we use an approximate, empirically based approach to analyze how the major environmental controls on sediment supply and transport might affect the stochastic regimes of sediment transport and routing in a channel network over long periods of time. The model leads to hypotheses that might be tested through temporal sampling of sediment flux and reach-length storage, spatial sampling of storage volumes throughout a channel network, space-for-time substitution, and reconstruction of sedimentation regimes after major environmental perturbations, such as fires, large storms, or land-use change. It is also useful for deducing testable interregional differences in the mean condition and variability of sediment storage and supply that might be expected to result from differences in climate, topography, and other landscape properties. The approach could also be used for anticipating the general nature of changes in sedimentation regime that might be expected to result from a change of climate, land use, or other resource management policy, such as fire suppression.

Similar to the approach taken in predicting the stochastic sediment supply [*Benda and Dunne*, this issue], we seek to avoid the complexities inherent in large-scale processes by using a coarse-grained approach [*Gell-Man*, 1994] that does not make precise predictions about future states at specific sites but uses simplified expressions to represent processes and their interactions. The approach is meant to generate testable hypotheses about the effects of interactions among climate, topography, lithology, and channel networks on large-scale patterns of fluvial sediment transport and storage.

2. Sediment Supply and Transport in the Central Oregon Coast Range

Certain aspects of the spatial and temporal behavior of sediment transport and storage at the scale of an entire river network are driven by long-term (decadal to millennial) hillslope erosion, which in the absence of land-use change varies with climate and topography. *Benda and Dunne* [this issue] developed a stochastic model of sediment production by landslides and debris flows in a 215-km^2 drainage basin in the central Oregon Coast Range (OCR) to investigate these effects. In that landscape, first- and second-order channels comprise approximately 90% of the cumulative channel length and they store colluvium for centuries [*Benda and Dunne*, this issue]. Episodic debris flows triggered by landsliding in bedrock hollows transfer this stored colluvium to higher-order valley floors. A stochastic model was used to compute the magnitude and timing of landsliding and debris flows, and thus of episodic sediment delivery to high-order channels (those with order $\geq$3). Although much of the sediment influx to high-order channels occurs continuously by soil creep and bank erosion, a pattern of infrequent wildfires and rainstorms coupled with a high density of landslide and debris-flow source areas causes a portion of the sediment supply to be concentrated in time and space [*Benda and Dunne*, this issue, Figure 3]. In the present paper we add to the computed sediment supply the rate of chronic soil creep from hillslopes lining the high-order channels, fluvial transport from first- and second-order channels, and the effects of sediment storage in debris-flow fans at the mouths of tributaries.

The wash load component of the sediment supply to these high-order channels is transported quickly downstream, and although a small fraction of it is trapped in gravely bed and bar material in the region and another fraction is stored overbank, we ignore these fractions in the current application. We also route the bed material within the active channel and ignore the construction of terraces and exchanges between terraces and the channel. Other strategies for characterizing these latter transfers have been suggested by *Dietrich et al*. [1982, pp. 15–20] and *Kelsey et al*. [1987]. We are concerned here with the sediment that travels episodically through the channel system as bed-material load and (although our one-dimensional model cannot distinguish between them) is molded into channel and floodplain forms. This sediment travels episodically in response to floods. The probability distributions of occurrence and distances of particle transport by these floods are generally unknown, but we take as reasonable the assumption that both are strongly right skewed and that the mean distance of transport per year is a small fraction of the length of the channel network [*Dietrich and Dunne*, 1978; *Madej*, 1982; *Mosley*, 1978].

In the present paper we compute a long-term (3000-year) sediment mass balance for channel reaches of third to sixth order in a 215-km^2 watershed in the central OCR using (1) the computed time series of sediment supply [*Benda and Dunne*, this issue], (2) field estimates of sediment storage in debris-flow fans and terraces, (3) laboratory measurements of particle abrasion, and (4) a mass balance sediment-routing procedure with a stochastic component to reflect temporal variability in flood hydrology and channel-bed state. The significance of particle abrasion is likely to vary strongly between different lithologic regions; it is considerable in the central OCR because the Tyee Sandstone of the region is exceptionally weak.

3. Stochastic Model of Fluvial Sediment Transport

3.1. High-Order Channel Network

Benda and Dunne [this issue] partitioned the 215-km^2 North Fork of the Smith River basin in the OCR into 1 km^2 grid cells to parameterize the density and topology of bedrock hollows and first- and second-order channels and to simulate wildfires and resultant mass wasting. In the fluvial routing model described here, we partition the high-order network into reaches (length 200–2500 m; average 800 m) between tributary junctions and grid cell boundaries (Figure 1), and we calculate sediment influx to each of these reaches from its local drainage area. Each channel reach is identified by its position in the

network, and its cumulative and local drainage areas, gradient, channel width, and hydraulic roughness are all specified. For purposes of bed load routing, each reach is divided into segments of length equal to the computed average annual distance of bed-particle transport in each part of the network. This is required so that we can calculate where sediment is stored or scoured along the channel as a result of the imbalance between sediment supply and transport within a segment.

3.2. Sediment Supply to High-Order Channels

Figure 2 illustrates the annual sediment mass balance for a segment of third or higher order in the channel network:

$$Q_i(k, t) + I(k, t) - Q_o(k, t) = \Delta V_t(k, t)/\Delta t \qquad (1)$$

where $Q_i(k, t)$ and $Q_o(k, t)$ are, respectively, the fluvial input (suspended wash load and bed load) from upstream and the fluvial export ($m^3\ yr^{-1}$) for segment k in year t. The sum of all distributed lateral inputs, $I(k, t)$ in $m^3\ yr^{-1}$, is computed for an entire reach (Figure 2) and is then distributed between all segments in the reach according to their length. The value $I(k, t)$ includes stochastically generated landslides, debris-flow, and fluvial scour from bedrock hollows and first- and second-order channels; soil creep from hillslopes along each reach; landslides from bedrock hollows that empty directly into the reach (approximately 12% of all hollows in the basin); and bank erosion of debris fans and terraces. The term $\Delta V_t(k, t)$ in cubic meters is the annual change of sediment storage within the segment, and Δt is 1 year. The term I includes the stochastic, spatially distributed sediment influx computed by *Benda and Dunne* [this issue], and because of its hillslope source and characteristic texture, we will refer to it as colluvium in this paper.

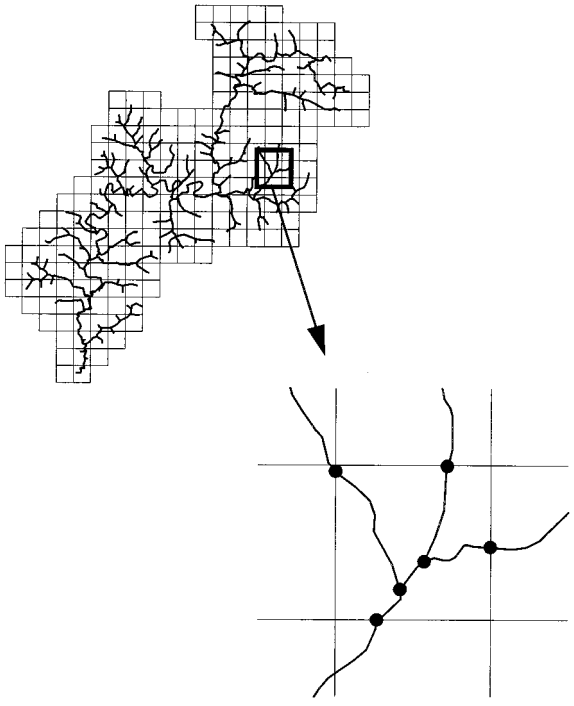

Figure 1. The third- and higher-order drainage network of the 215-km^2 basin of the North Fork Smith River showing the placement of 1-km^2 grid cells and the definition of channel segments (bounded by dots) between grid cell boundaries and third- and higher-order channel junctions.

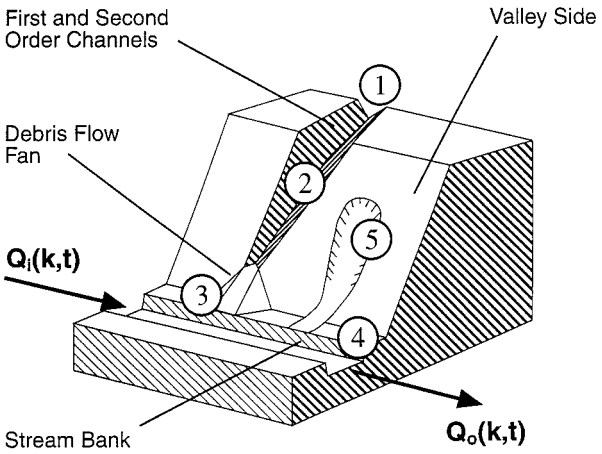

Figure 2. An illustration of the sediment mass balance of third- and higher-order channel segments in the simulation model. The annual fluxes of bed load and suspended load into and out of the kth segment in year t are indicated by $Q_i(k, t)$ and $Q_o(k, t)$. Other processes include (1) shallow landsliding and debris flows in first- and second-order channels, (2) fluvial erosion and transport in first- and second-order channels, (3) bank erosion of debris-flow fans and terraces, (4) soil creep along toeslopes of hillsides, and (5) landslides from streamside hollows.

The volume of debris-flow sediment entering the high-order network each year is modified to account for the effect of storage in debris-flow fans or terraces in the valley floor [*Benda*, 1990]. Debris flows in the OCR typically deposit a portion of their sediment on debris fans at tributary junctions. Those entering third-order channels from upstream create large terraces along the valley floor. Stream erosion along the margins of these fans and terraces remobilizes the sediment. Field measurements of the initial failure, scour, and deposit volumes for five debris flows in the OCR occurring between 1983 and 1985 documented the deposition of 10–60% (average 40%) of debris-flow volumes on fans at the mouths of first- and second-order basins. Less-precise observations on older deposits, for which it was more difficult to define the scour volumes, suggested that the upper end of this range was more typical of the region, and so an average storage volume of 60% was used. Use of this proportion to calculate debris-flow deposit volumes and thicknesses in third-order channels was consistent with observed depths. Similar reconstructions of debris-flow volumes and deposition on terraces in the upper ends of third-order reaches indicated that an average of 75% (50–80%) of the original debris-flow volume was stored on terraces. These estimates were conservative in the sense that they exceed the averages of the more precisely measured values, and thus they diminish the predicted initial amplitude of colluvial deposition in the channels. However, it is clear that a larger database is required to investigate this aspect of channel and valley-floor sedimentation.

As a consequence of this estimate of fan and terrace storage, we applied an average, constant rate of stream bank erosion of 0.02 m yr^{-1} along the streamside margins of debris-flow fans at the mouths of first- and second-order channels and an erosion rate of 0.06 m yr^{-1} along debris-flow terraces in upper third-order valleys. These values were chosen to maintain the storage reservoirs in long-term steady state, based on the average frequency and volume of debris flows predicted by *Benda and*

Dunne [this issue]. Future measurements of interannual variability of bank erosion rates or storage volumes may allow definition of another stochastic component of the sediment budget.

The model thus computes a sediment supply rate in each of the grid cells in each year and records the volume of colluvium originating from the portion of each grid cell that drains directly into each high-order channel segment (Figure 1).

3.3. Texture of Sediment

The particle-size distribution of colluvium is similar among hollows and first- and second-order channels [*Benda and Dunne*, 1987], showing that low-order channels trap sediment of all sizes, including almost all of the sand and silt from hillslopes, until that sediment is scoured away by debris flows. The particle-size distribution (by weight) of sediment that enters channels of all orders from all erosion processes is 6% silt-clay (<0.06 mm), 8% sand (0.06–0.25 mm), 7% coarse sand (0.25–1 mm), 18% pebbles (1–22 mm), 18% gravel (22–64 mm), 35% cobbles (64–264 mm), and 8% boulders (>264 mm). Many of the pebbles are cemented sands, which break down rapidly during wet sieving or tumbling. The distribution is based on field measurements of colluvium from bedrock hollows and debris-flow deposits in the OCR.

Bed load in our model includes all particles smaller than boulders (i.e., <264 mm) and greater than fine sand (0.25 mm), which is the upper limit of suspended load in OCR streams [*Beschta*, 1981]. Sediment finer than 0.25 mm is assumed to remain in suspension as wash load. In the model, boulders remain at depositional sites [*Benda*, 1990] and weather to sand and gravel during periods between debris flows, which average 600 and 300 years, respectively, for first- and second-order channels [*Benda and Dunne*, this issue].

3.4. Sediment Routing Model

A mass balance approach (equation (1)) is used for routing sediment through the approximately 300 km of high-order channels over a 3000-year period. We distinguish between wash load (<0.25 mm), which is rare in the bed material of the field area and is exported from the basin once it is separated from colluvium, and coarser sediment that travels dominantly as bed load. A portion of the wash load may be temporarily stored overbank in floodplains or terraces [*Madej and Ozaki*, 1996], but since our observations in the field area indicate that floodplain material in most reaches of the network is coarse, especially in the upper reaches of the basin, we ignore floodplain storage of wash load in the present application. Sediment stored in the active channel and in coarse-textured floodplains of the basin is always available for transport in the calculation, and therefore longer residence times of sediment in valley-floor stores [*Dietrich and Dunne*, 1978] are not accounted for in this one-dimensional model. A change in sediment supply is often accompanied by an adjustment in channel morphology, including bed particle size [*Dietrich et al*., 1989] and pool-riffle geometry [*Lisle*, 1982]. These changes in morphology in turn can affect the sediment transport rate, but in the absence of quantitative relations, these feedbacks are not represented in our model.

In the absence of a physically based sediment transport equation that is well proven for mountain channels and of knowledge of particular sequences of flow to drive such an equation, we take a stochastic approach to estimating annual transport rates. Our approach is based on (1) the common experience that probability distributions of annual sediment fluxes at a station are right skewed [*Wolman and Miller*, 1960; *Van Sickle and Beschta*, 1983], (2) an empirical estimate of the mean and variance of this probability distribution, and (3) field verification that the mean annual transport distance for bed load particles is a small fraction of the channel network length. We emphasize the approximate nature of such a transport estimate, but we are interested in exploring consequences of the imbalance between transport and the spatially and temporally discrete packages of sediment that are supplied to the channel network under the stochastic conditions of basin-wide erosion described by *Benda and Dunne* [this issue]. We employ only an approximate form of the transport probability distribution under realistic field conditions to avoid uncertainties in sediment transport theory for mixed-grain transport in rough mountain channels, limited data on network-wide channel conditions, and the unpredictability of streamflow. This module of the approach can be improved independently for other applications according to the availability of measurements or theoretically tractable transport conditions.

We begin by defining an annual total transport volume out of a segment under conditions of copious sediment supply, $\eta(k, t)$, which varies between years (t) and channel segments (k) and has dimensions of ($m^3\ yr^{-1}$). Its probability distribution will be estimated below. Subtraction from η of the computed washload input to the segment $Q_{iw}(k, t)$ leaves $\Psi(k, t)$, the sum of wash load that is mobilized within the segment and bed load that is transported out of the segment k in year t:

$$\Psi(k, t) = \eta(k, t) - Q_{iw}(k, t). \tag{2}$$

We propose that under conditions of copious sediment availability, the partitioning of Ψ between bed load transport through the segment and new suspension within it will be proportional to the ratio of the volumes of suspendible to total sediment within the segment. Thus, with copious sediment supply, $\vartheta_w(k, t)$, the wash load ($m^3\ yr^{-1}$) mobilized within the segment would be

$$\vartheta_w(k, t) = \Psi(k, t)[V_w/V_t] \tag{3}$$

where V_w (cubic meters) is the volume of wash load in colluvium supplied to the segment from its local drainage area and V_t (cubic meters) is the total volume of sediment stored within the segment in year t, which may consist of colluvium supplied from the local drainage area and alluvium supplied from upstream in year t or earlier years.

Under a restricted sediment supply, if the amount of washload grain sizes stored in the reach in a particular year is less than $\vartheta_w(k, t)$, then all of this fine-grained material will be flushed out of the segment, and the annual volume of wash load mobilized within the segment will be

$$\kappa_w(k, t) = V_w(k, t)/\Delta t. \tag{4}$$

Otherwise, $\kappa_w(k, t) = \vartheta_w(k, t)$ from (3). Hence the total wash load transported out of segment k in year t, $Q_{wo}(k, t)$ is

$$Q_{wo}(k, t) = Q_{wi}(k, t) + \kappa_w(k, t) \tag{5}$$

where $Q_{wi}(k, t)$ is the wash load transported into the segment. Once wash load is suspended, it remains in motion and leaves the basin in the same year, so that in high-order channels only colluvium contains particles smaller than 0.25 mm.

Under a copious sediment supply the annual flux of bed load out of a segment is also partitioned from $\Psi(k, t)$ according to

the proportion of bed load–size material, V_b, (which includes that supplied from upstream during the previous year and that supplied by colluvium from the local drainage area) to the total sediment volume, V_t, stored in the segment:

$$\vartheta_b(k, t) = \Psi(k, t)[V_b/V_t]. \quad (6)$$

Under a restricted sediment supply, if the volume of bed load particles stored in the reach in a particular year is less than $\vartheta_b(k, t)$, then all of this material will be flushed out of the segment, and the annual volume of bed load mobilized within the segment will be

$$\kappa_b(k, t) = V_b(k, t)/\Delta t. \quad (7)$$

Otherwise, $\kappa_b(k, t) = \vartheta_b(k, t)$ from (6). Hence the total bed load transported out of segment k in year t is

$$Q_{bo}(k, t) = \kappa_b(k, t). \quad (8)$$

Equations (2) and (6) lead to the condition that under copious sediment supply, computed values of bed load vary according to the supply of suspended sediment from upstream. We use this result only in the sense of the difference between two randomly varying numbers. It is a consequence of using a probability distribution of measured sediment yields including both suspended and bed load sediment to estimate η, then of subtracting from the values for individual years an independently predicted wash load, and of assuming that all wash load, once mobilized, is never redeposited. In short, it is a result of the fundamental uncertainty acknowledged in our use of a probability distribution in the first place. Although there is room for improvement in this module, the flaw makes very little difference to the results in the present application. The total transport (η) increases monotonically downstream with increasing drainage area, whereas bed load breaks up rapidly by abrasion because of the mechanically weak bedrock of the region (see below), so that $\vartheta_b(k, t)$ almost always exceeds the amount of bed material that arrived in a segment during the previous year. Therefore once bed load is in motion (i.e., separated from its originating colluvial deposit), it continues to move downstream each year. The dependence of $\vartheta_b(k, t)$ on the flux of suspended load from upstream artificially slows the calculated erosion of colluvial deposits by reducing stream erosion of the deposit during high fluxes of suspended load from upstream. The expected strong right skew in the predicted frequency distributions of annual bed load transport is preserved [e.g., *Benda*, 1994, p. 234].

3.5. Probability Distribution of Sediment Transport Rates

In order to simulate the stochastic effects of flood hydrology and of variations in channel bed conditions on sediment transport, we estimated the probability distribution of total annual flux (η) from measurements of sedimentation in reservoirs and from sampling suspended load at stations with drainage areas ranging from 0.7 to 1523 km^2 over periods of 2–18 years [*Reneau and Dietrich*, 1991]. The bed load contributions were likely to be at most several percent of the total load in these short-term measurements [*Brown and Krygier*, 1971; *Beschta*, 1981; *Collins and Dunne*, 1989]. We used measurements from periods of significant watershed disturbance due to timber harvest and road construction in eight of the basins to compute a regional mean sediment transport rate of 150 t km^{-2} yr^{-1} (140 m^3 km^{-2} yr^{-1}) ± 31 t km^{-2} yr^{-1} (standard deviation) that we took as representing conditions of copious sediment supply. Since there was no variation with drainage area over the range 0.7–1523 km^{-2}, we applied the value of 150 t km^{-2} yr^{-1} to each segment in the channel network to obtain its long-term mean sediment transport rate under conditions of copious sediment supply.

The probability distribution of annual transport rates at a station was obtained from measurements in two logged Alsea basins (0.7 and 3.0 km^2) for which 16 station-years of annual yields [*Brown and Krygier*, 1971; *Beschta*, 1978] were approximately lognormally distributed with a logarithmic mean of 145 t km^{-2} yr^{-1} and a standard deviation of 0.24 log units. Thus for each year of the simulation a value is selected randomly from a lognormal probability distribution of η values with a mean of 150 t km^{-2} yr^{-1} and a standard deviation of 0.24 log units, and is scaled to the total drainage area of the 370 reaches for use in (2) through (8); all segments (Δx) contained in each reach have the same η. There were 2960 segments in the computation.

We do not imply that the simulated sediment transport rates under copious sediment supply represent the transport capacity in the presence of an infinite sediment supply. Use of a probability distribution of η expresses not only variations in sediment transport due to alternations of wet and dry years but also the temporal variation of land cover and other processes affecting the availability of sediment in a basin, as well as the state of the channel bed. Thus it expresses our lack of knowledge about the annual sediment transport rate, except for the empirical record of its general magnitude and variability.

3.6. Average Distance of Bed Load Transport

Each segment was assigned a length, $\Delta x(k)$, equal to the average annual distance of bed-particle transport estimated for that place in the channel network, so that we could keep track of the transport distance of each year's bed load. Travel distance depends on the average particle speed during transport and the duration of floods and of burial. Field measurements of tagged bedload particles show only weak dependence of travel distance on size [*Hassan and Church*, 1992; *O'Connor*, 1993], so particle size of bed load is omitted from our transport model. We developed and calibrated a method for estimating the average particle speed by following the suggestion of *Bagnold* [1954] that the work rate involved in bed load transport (i_b, W m^{-2}) is related to stream power expenditure (ω, W m^{-2}) by an efficiency factor (e_b) that expresses the bed load speed as some fraction of the flow speed.

Bagnold [1954] expressed the power requirement for continuous bed load transport in terms of the immersed weight of the moving sediment, particle speed, and a friction coefficient:

$$i_b \tan \phi = [(\rho_s - \rho_w)/\rho_s] m_b g v_b \tan \phi \quad (9)$$

where $\tan \phi$ is the dynamic friction coefficient, which [*Bagnold*, 1954, 1973] is variously evaluated as 0.63–0.75; ρ_s and ρ_w are respectively the densities of particles and water (kg m^{-3}); m_b is the bed load mass per unit area of channel bed (kg m^{-2}); g is the gravitational acceleration (m s^{-2}); and v_b is the mean bed-particle speed (m s^{-1}). This power requirement is met by the expenditure of stream power per unit area of bed modulated by an efficiency factor, e_b:

$$i_b \tan \phi = \omega e_b = e_b \tau v_f = e_b \rho_w g h s v_f \quad (10)$$

where τ is the total bed shear stress (N m^{-2}), v_f is the mean flow velocity (m s^{-1}), h is average bankfull flow depth (meters), and s is the channel gradient. Thus

$$[(\rho_s - \rho_w)/\rho_s]m_b g \tan \phi v_b = \rho_w g h s v_f e_b \quad (11)$$

and during bed load transport the particle speed should depend on characteristics of the flow and the sediment in transport

$$v_b = [\rho_s \rho_w/(\rho_s - \rho_w)](hs v_f \tan \phi)(e_b/m_b) \quad (12)$$

Field measurements by *Beschta* [1981] at drainage areas of 2–3 km^2 in the OCR indicated that bed load transport occurs almost entirely near bank-full stage, which lasts for approximately 0.3% (1 day) of each year, allowing conversion of particle velocities in (12) from m s^{-1} to m yr^{-1}.

For the calculation of bank-full flow depth and velocity in each segment we first estimated the 1.5-year flood as a function of drainage area for Pacific Slope basins in Washington State that are similar to those of the OCR [*Bodhaine and Thomas*, 1964]. Then we calculated flow depth and velocity from Manning's equation by using empirical basin-wide relationships that we developed [*Benda*, 1994] among drainage area and channel gradient (from 1:24,000-scale maps), bank-full width (from field measurements), and hydraulic roughness (from visual estimates using the method of *Barnes* [1967]).

During periods of copious sediment supply we have observed that bed material in the North Fork Smith River basin is scoured to depths of up to 1 m during floods, and under more stringent sediment supply the bed material is scoured to bedrock at depths of approximately 0.1 m, the D_{90} of thin sheets of gravel. There may be an inverse relationship between the depth of mobile material and the efficiency parameter in (12). However, in the absence of much knowledge of these values, and for purposes of illustration only, we used an average entrainment depth of 0.5 m (m_b = 600 kg m^{-3}) and an efficiency of 0.05, which lies in the range of values for gravel measured by *Leopold and Emmett* [1976]. This choice yields bed-particle speeds of about 140 m yr^{-1} at a drainage area of 10 km^2 and about 100 m yr^{-1} at 50 km^2 in the North Fork Smith River, although the potential range is from a few tens to a few hundreds of meters per year.

The reasonableness of such values is confirmed by an independent estimate. We calculated the long-term average bed-particle speed through high-order channels in the basin by dividing the volume of material stored in each segment (measured in the field) by the throughput of bed material computed from the measured sediment yields referred to earlier and an average bed load/total load ratio predicted by the model for each segment [*Benda*, 1994, p. 136]. The method predicted average particle speeds of 26–325 m yr^{-1} with a mean of 130 m yr^{-1}. These results are similar to the calculation of 236 m yr^{-1} for bed material in a fourth-order reach of another basin in the OCR [*Dietrich and Dunne*, 1978] and to a tracer-particle speed of 234 m yr^{-1} measured by *Milhous* [1973] for a gravel-bedded stream in western Oregon. *Hassan and Church* [1992] and *Church and Hassan* [1992] summarized field studies of tagged gravel particles, indicating maximum travel distances less than 350 m for large flow events, with the majority of travel distances less than 200 m. With this sparse support for the reasonableness of our computed bed-particle speeds, we used (12) and

$$\Delta x(k) = v_b(k)\Delta t \quad (13)$$

to set the length of each segment in the channel network.

3.7. Particle Abrasion

Abrasion of bed material during transport reduces all coarse particle sizes, but most important for the present calculation is the conversion of bed material to wash load. The process has been simulated by tumbling sediment in a mill and expressing the resulting particle size as an exponential function of simulated travel distance [e.g., *Collins and Dunne*, 1989] with the e-folding distance of the exponential function depending on lithology. The Tyee sandstone of the central OCR is mechanically weak, and so conversion of bed material to wash load is particularly rapid. Since it is not practical to account for the movement and burial history of each particle in the channel network, we ignored the potential for a grain-size dependency on abrasion rate, and focused only on determining the proportion of the bed material that would be converted to washload as it traveled through each channel segment.

Bed load abrasion was measured by tumbling colluvium in a water-filled, rubber-lined drum at a rotation rate of 0.2 m s^{-1} [*Benda*, 1994]. The bed load–size component in the colluvium decreased dramatically as cemented aggregates and weathered rock, especially in the 1- to 4-mm size class, disintegrated. An equation of the form

$$V_x = V_i e^{-\xi x} \quad (14)$$

was fitted to the tumbling results, where V_x is the volume of bed-material-size particles after a distance of travel, x; V_i is the volume of those particles in the original material; and ξ (km^{-1}) is the abrasion resistance parameter. A value of 0.2 km^{-1} for ξ reproduces the abrasion rate estimated by the tumbling mill in the first 5 km, whereas ξ = 0.1 km^{-1} more closely represents the abrasion from 15 to 25 km [*Benda*, 1994]. Because the tumbling mill does not account for weathering of gravel during storage in channels, the higher rate (ξ = 0.2 km^{-1}) was used in the simulations. These are probably exceptionally high values compared to analogous measures for other lithologies.

This exponential abrasion rule was implemented by means of the equation

$$Q_{bo}(k, t)\Delta t = Q_{bi}(k, t)\Delta t[1 - \xi \Delta x(k)] \quad (15)$$

where $Q_{bo}(k, t)$ and $Q_{bi}(k, t)$ are respectively the volumes of bed material leaving and entering segment k in year t, and $\Delta x(k)$ is the distance of particle travel (the length of segment k). Suspended load generated by the abrasion of bed load in a segment is added to the suspended load leaving the segment.

3.8. Storage in Each Channel Segment

The amount of sediment in storage in a channel segment at the end of year t can be expressed as a volume per unit area of channel bed and therefore as an average depth of stored sediment, z:

$$z(k, t) = \{[Q_{bi}(k, t) - Q_{bo}(k, t)]\Delta t + I(k, t)\Delta t + V_t(k, t - 1)\}/w\Delta x(k) \quad (16)$$

where $V_t(k, t - 1)$ is the volume of colluvium and alluvium in the segment that survived previous stream erosion (from mass wasting or tributary inputs which overwhelmed the transport capacity of the stream in the segment) and w is the channel width.

The model does not include the ability of woody debris to trap colluvium and alluvium upstream, as described by *Benda* [1988, 1990] for the OCR, by *Perkins* [1989] for the Washington Cascade Range, and by *Megahan* [1982] for Idaho. Our field observations in Harvey Creek (referred to below) and the Tillamook basin in the OCR indicate that large influxes of

sediment resulting from episodes of fire and mass wasting of the kind modeled by *Benda and Dunne* [this issue] bury jams of organic debris. The integrated effects of woody debris are presumed to be represented in the probability distribution of sediment transport rates estimated from the reservoir and sampling data.

3.9. Steps in the Simulation

The stochastic sediment generating scheme described by *Benda and Dunne* [this issue] was used to compute an annual time series of sediment influx to each segment of the high-order channel network. These values, $I(k, t)$, separated into wash load and bed load size components, are used in (1) to calculate both storage of sediment within the segment and sediment flux out of it in each year. Calculation of the efflux, $Q_o(k, t)$, requires first the random selection of an annual value of total transport for year t from the probability distribution of η and its scaling for each segment based on drainage area. The efflux is then partitioned into wash load and bed load with (5) and (8), respectively. Wash load leaves the basin and generates a time series in which the suspended load is more or less decoupled from the slower bed load. Each year's bed load travels a distance equal to the length of the next segment downstream, computed from (13) and in doing so is diminished in volume by particle abrasion (equation (15)), which also yields a time series of bed load flux for each segment. Equation (16), which is an expanded version of (1), is then used to calculate a time series of sediment storage for each segment in the basin.

4. Model Results and Discussion

4.1. Nonuniform and Unsteady Sediment Supply

We are now in a position to use the simplified transport model to investigate how the space-time structure of sediment routing and storage is governed by interactions between the stochastic supply of sediment from hillslopes and a converging, hierarchical channel network. The simplicity is required to overcome the complexities introduced by long time periods and large ensembles of hillslopes and channel reaches. The result is a set of hypotheses on how the large-scale behavior of erosion and sedimentation is related to specific environmental variables.

Much of the sediment supply shows little interannual variability because soil creep and fluvial transport from low-order channels are chronic processes, and most of the colluvium supplied by landslide and debris flow is initially stored in fans and terraces and removed gradually by bank erosion. However, climatically driven perturbations in the form of wildfires and rainstorms, coupled with a high density of landslide and debris-flow source areas, result in a portion of the sediment supply being strongly nonuniform and unsteady [*Benda and Dunne*, this issue].

During full simulations of these interactions it is difficult to observe the movement of sediment downstream from a single hillslope source because of the numerous hillslope and streamside sediment sources in the basin, mixing of sediment at tributary junctions, and particle attrition. To illustrate routing of sediment through a portion of the network, we first simulated the response of sediment transport and storage to a single hypothetical, small fire covering 4 km^2 near the head of the North Fork Smith River.

In the computed example, landslides and debris flows deposit 26,000 m^3 of colluvium into an 800-m-long, 3-m-wide, third-order channel reach (drainage area = 4.6 km^2; slope = 0.016). Accelerated deposition persists for 4 years because of the succession of rainstorms during the period of declining root strength and includes no other landslides or debris flows from upstream, although there is a chronic sediment supply from soil creep, bank erosion, and fluvial erosion from low-order channels upstream of the third-order reach. A portion (60%) of the landslide and debris-flow volume is deposited in fans and terraces to be removed by later bank erosion. The remainder consists of colluvium scoured from hollows and channels of first and second order and deposited in the third-order channel with little sorting by the debris flow. The deposit in this case is initially 4.0 m thick. Field observations of such deposits indicate that they are poorly sorted, containing boulders and copious suspendible sediment, and they remain in the channel as stationary waves with distinctive granulometry, which in this paper we refer to as colluvium.

After the period of accelerated mass wasting, the simulated sediment transport from the reach reverts to the condition in which $Q_o(k, t) > [Q_i(k, t) + I(k, t)]$, implying degradation of the deposit. The time required for the third-order stream to erode the 4-m-thick deposit of colluvium in the simulated example is controlled by (1) the initial volume of sediment supplied to the channel by mass wasting (i.e., hillslope supply minus fan and terrace storage) and by fluvial transport from first- and second-order channels; (2) the annual time series of sediment transport rates ($\eta(k, t)$); (3) the supply of suspended load into the channel segment from upstream of the deposit, $Q_{wo}(k - 1, t)$, that affects the magnitude of the remaining sediment transport rate ($\Psi(k, t)$) and therefore the rate at which the stream erodes the colluvium; and (4) the supply of bed material into the reach from upstream, $Q_{bo}(k - 1, t)$. In the simulated case the degradation time is 20 years. The complicating effects of temporal changes in channel morphology, including armoring and woody debris, on sediment transport were not explicitly considered, except through the strategy of using the empirically derived probability distribution of transport rates.

Stream erosion of the stationary colluvial wave produces a pulse of suspended sediment, which exits the basin in the first few years after onset of the disturbance, and a pulse of fluvially transported bed material, which moves downstream through a channel that is usually limited in sediment supply (i.e., transport capacity exceeds supply of sediment) prior to the accelerated erosion. In coarse-bedded, steep channels the bed material moves almost exclusively as bed load, and so we will use these terms interchangeably in the rest of this paper. The mobile pulse of fluvially transported bed material is more sorted than the stationary colluvial deposit, and it is to these mobile features that we apply the term "wave" in the rest of this paper, unless there is specific reference to the stationary colluvial waves. In this case the pulse of bed material moves as a coherent wave (Figure 3), the translation and alteration of which are computed by application of (16) to successive channel segments and successive years. A bed-material wave is therefore defined as a region of relatively high sediment transport and storage bordered upstream and downstream by zones of lower transport and storage.

The initial volume of the bed load pulse is controlled by the volume of bed load–size material in the initial influx of colluvium. The length of the wave is the average annual particle speed multiplied by the duration of the period in which bed-material outflow exceeds inflow in the original third-order

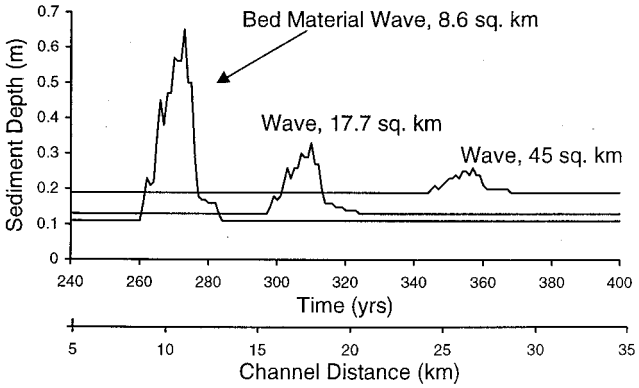

Figure 3. Spatial and temporal change of a simulated bed-material wave that originated from a single small fire at the head of the North Fork Smith River; all other fires were suppressed.

reach affected by accelerated mass wasting. In the simulated example the average annual bed load travel distance of approximately 0.15 km yr^{-1} and the duration of degradation of the deposit (20 years) yield a pulse length of approximately 3 km in Figure 3. Measured velocities of sediment waves include 0.15 km yr^{-1} (M. D. O'Connor and T. W. Cundy, unpublished report, 1993), 0.5 km yr^{-1} [*Beschta*, 1984], and 0.7–1.6 km yr^{-1} [*Madej and Ozaki*, 1996], values which are essentially analogous to our travel speeds because diffusional effects on wave speed are small in our calculation.

We have illustrated the case in which the travel distances of particles show relatively little dispersion, and therefore there is little diffusion of the wave. Our model incorporates diffusion only where there is a downstream increase in particle travel speed, either at a tributary junction because of discharge increases or at a narrowing or steepening of the channel, which is excluded in this application by our estimation of gradient as a smooth function of drainage area. Where such an increase in particle speed occurs, the segment length in our calculation increases (equation (13)) and the sediment entering the reach in a year is spread over a larger Δx in (16). In other words, some diffusion of the wave would be forced by the dispersion of particle velocities in a reach where the speed increased. Field measurements of particle travel distance [e.g., *Hassan and Church*, 1992] indicate that some dispersion of particles is to be expected under certain conditions of grain-size composition and hydrograph characteristics, but because this mechanism is weak and not yet well understood, we have chosen to approximate transport distances as a single value for each position in the network and therefore probably to underestimate the effects of diffusion. Where wave diffusion is important, it will result in wave amplitude decreasing downstream faster than is accounted for here, and individual waves may coalesce faster into extensive gravel trains. If the wave is thinning while traversing a long, sediment-starved reach, it may eventually be manifested as a patch of relatively fine-textured bed with coarser bed or bedrock upstream and downstream [*Collins et al.*, 1994, p. 81].

Another case is that in which sediment is stripped from the initial colluvial wave in small quantities and transported quickly downstream without aggrading the bed until it is transported to some reach in which the transport capacity decreases and the sediment accumulates. This accumulation would continue until the supply of sediment from the colluvial wave diminishes, and then the downstream deposit would be scoured away. Thus the initial colluvial influx would be partially converted to a stationary fluvial wave at a remote locality downstream (such as the mouth of a canyon). This process could be repeated along rivers with alternations of high and low gradient, and a patient observer would see waves of sediment storage arising and decaying with some lag and particle-size change as a result of the initial massive influx of sediment in a zone of the basin in which sediment supply had been increased in the recent past.

Because of the difficulties of modeling sediment transport capacity in sediment-starved channels, we have limited our model to the simplest conceivable case of bed-material flux without dispersion. Thus we hope to concentrate attention on our main points, namely, (1) that stochastic sediment supply from massive fires and rainstorms and the effects of channel network topology focus that sediment supply spatially and temporally to create transient zones of sediment storage along the channel network and (2) that this transient behavior has a spatial and temporal structure that can be related to environmental variables.

Particle attrition causes a loss of mass in the sediment wave as it moves downstream. Wave height, from (16), is also reduced downstream because of increasing channel width (Figure 3). Although the bed material waves appear dramatic in Figure 3, they are subtle features having amplitudes of several decimeters to several meters (in examples shown later and in the field area) and lengths of tens of meters to several kilometers prior to wave mixing or to diffusion by particle dispersion or attrition. The high-frequency variation in the waveform (Figure 3) is due to the annual variation in flood flows, which is represented in our model by the sampling of total transport rates (η) from a probability density function. The increase in depth of sediment between waves with increasing drainage area (Figure 3) results from sediment supplied by continuous erosion processes occurring throughout the watershed.

Sediment waves having durations of seasons to years occur in channels of a variety of sizes worldwide [*Gilbert*, 1917; *Mosley*, 1978; *Griffiths*, 1979; *Pickup et al.*, 1983; *Meade*, 1985; *Nakamura*, 1986; *Roberts and Church*, 1986; *Jacobson*, 1995; *Madej and Ozaki*, 1996]. Our goal in the latter part of this paper is to illustrate the characteristic frequency, magnitude and spatial distribution of wave-like sediment transport in the context of climatic perturbations, basin topography, network topology, and the movement history of waves.

4.2. Frequency and Magnitude of Sediment Transport and Storage

The frequency and magnitude of sediment supply to high-order channels increase downstream because the number of landslides and debris-flow sources and of wildfires multiply with increasing drainage area [*Benda and Dunne*, this issue, Figure 12]. The consequences of the predicted space-time structure of erosion on the temporal behavior of sediment storage and routing, and channel morphology are examined in channel reaches with drainage areas of 3, 25, and 215 km^2, in third, fifth, and sixth stream orders, respectively.

The predicted 3000-year time series of sediment depths (including bed material and colluvium) in a third-order channel segment (drainage area = 3 km^2; $s = 0.02$) exhibits centuries of thin sediment cover on the channel bed and supply-limited transport conditions punctuated by decades of deep sediment and transport-limited conditions (Figure 4a). The supply-

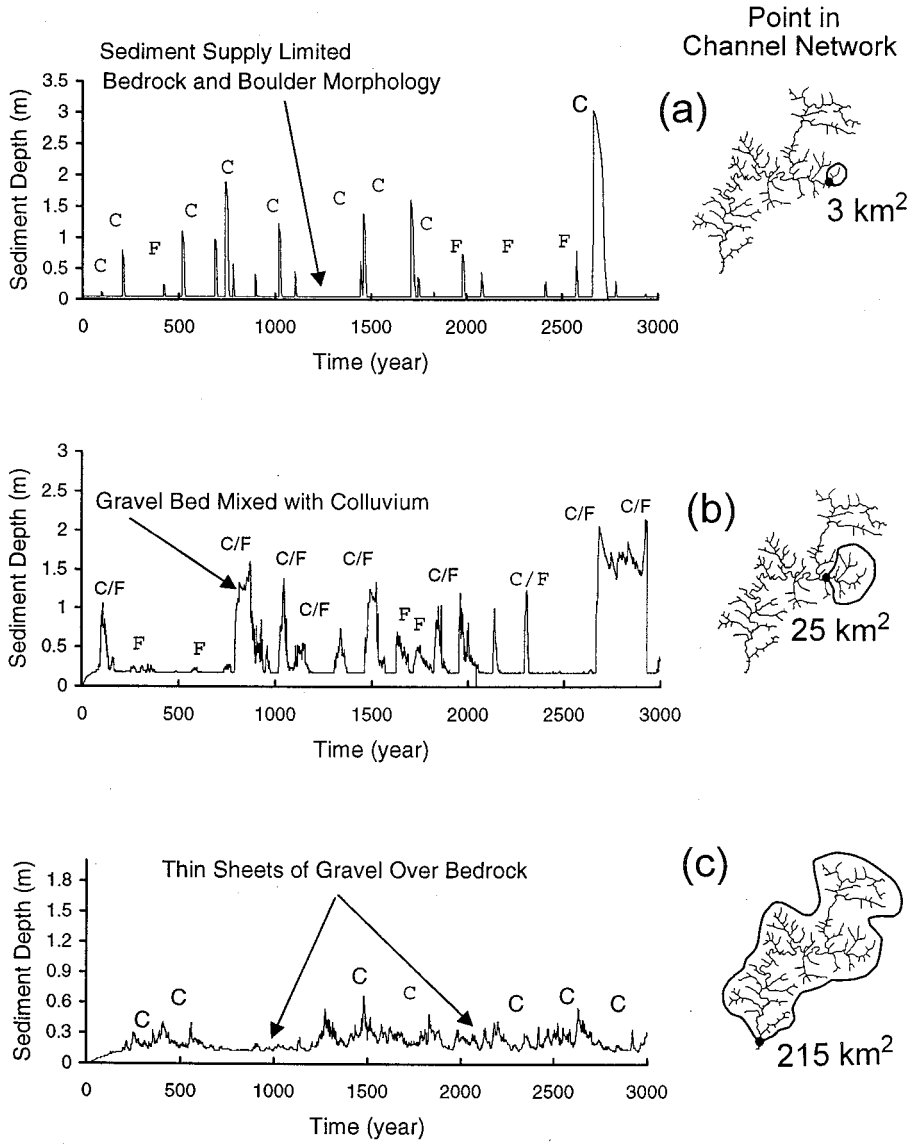

Figure 4. The predicted time series of sediment depths (including colluvium from landslides and debris flows, and fluvially transported sediment) in (a) a third-order channel draining 3 km^2, (b) a fifth-order channel draining 25 km^2, and (c) a sixth-order channel draining 215 km^2. "C" and "F" represent, respectively, sediment associated with colluvium (from mass wasting) and fluvially transported sediment. Only the largest signals in the series are denoted. The 250-year-long wave in the fifth-order channel results from an extended period of frequent landsliding that caused repeated mixing of colluvium with fluvial gravel waves. In the sixth-order channel, only the colluvium is indicated because the amplitudes of the fluvially transported waves are small. Field observations of channel morphology associated with different sediment depths are included.

limited periods, with average depth of channel substrate <0.1 m, result from sediment transport rates (both bed load and suspended load) equaling or exceeding the supply of sediment from the continuously occurring erosion processes in the watershed. Transport-limited conditions occur when landslides and debris flows, triggered by wildfires and storms [*Benda and Dunne*, this issue, Figure 3], deposit colluvium of local origin decimeters to a few meters deep (labeled "C" in Figure 4) in channels and temporarily overwhelm the stream's transport rate. Fluvially transported sediment waves (labeled "F" in Figure 4) also pass through the reach from upstream (average thickness = 0.6 m). These transient fluvial sediment waves are few, however, because of the limited number of debris-flow sources in a channel with a 3-km^2 drainage area.

In third-order channels of the OCR, limited bed material results in bedrock-floored channels with occasional boulders and accumulations of boulders at tributary junctions of first- and second-order channels [*Benda and Dunne*, 1987; *Benda*, 1990]. The exception is immediately behind woody debris, where gravel and sand accumulate, although this process does not alter the dominance of bedrock- and boulder-floored channels. The range of thicknesses of bed material predicted by the model (0.1–3.0 m) in this size of channel is similar to field measurements (0.0–2.0 m) in 20 channel segments having drainage areas between 3 and 10 km^2 in the central OCR [*Benda*, 1994]. Following deposition of colluvium by landslides and debris flows, the third-order bedrock channels at and downstream of the deposits are temporarily covered with

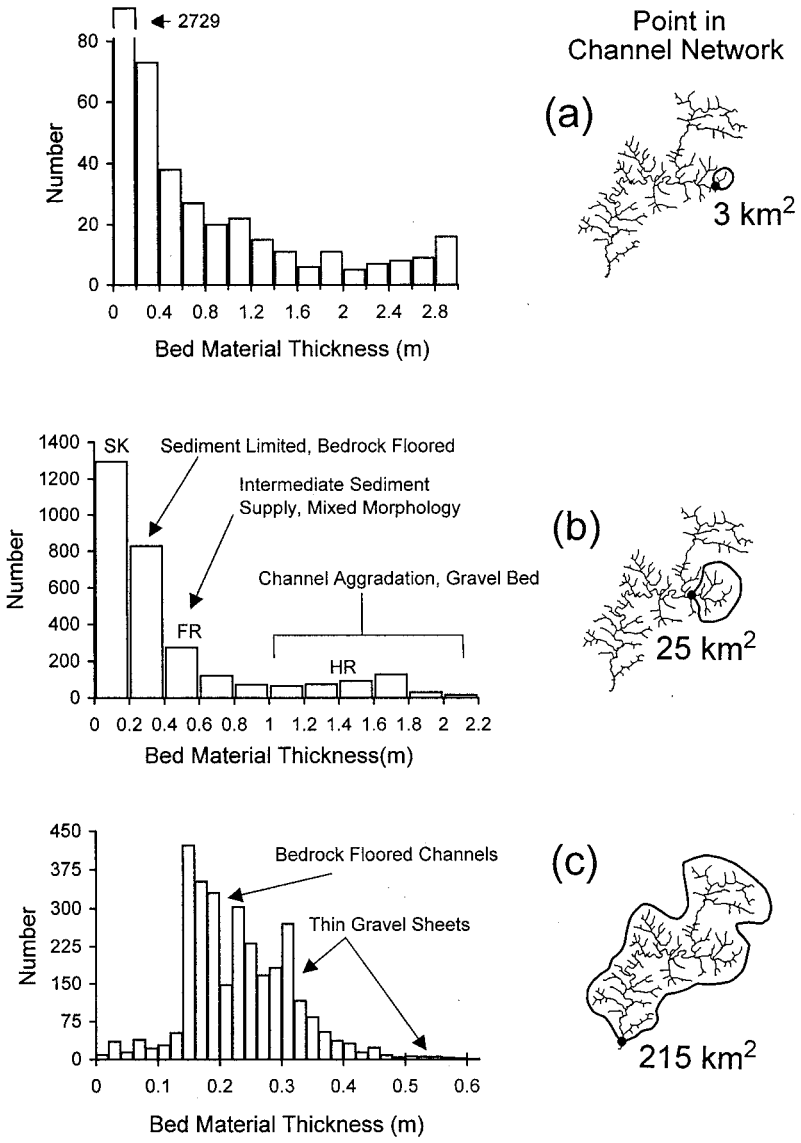

Figure 5. The predicted frequency distribution of sediment thicknesses derived from the time series in Figure 4 for channel segments with drainage areas of (a) 3 km^2, (b) 25 km^2, and (c) 215 km^2. Field observations of channel morphology associated with the different frequency distributions are included. "HR," "FR," and "SK" in Figure 5b denote the sediment supply condition for three field sites, Harvey, Franklin, and Skates Creeks, discussed in the text.

gravel beds. We have observed these gravel deposits downstream of debris flows in third-order channels in the OCR [*Benda*, 1990], and our model predicts that these deposits are relatively short lived (years to a decade), although debris jams can slow the routing of sediment [*Perkins*, 1989]. In addition, debris-flow deposits can constrict valley floors, temporarily creating ponds in certain locations of the network [*Everest and Meehan*, 1981; *Benda*, 1990].

The dominance of supply-limited conditions in the third-order channel segment is shown in the temporal frequency distribution of sediment thickness during the simulation (Figure 5a). The frequency distribution is approximately exponential, indicating that during most of the simulated history third-order channels are floored by bedrock or boulders and local deposits of boulders and cobbles. Channels containing gravel or cohesive, poorly sorted debris-flow deposits are predicted to occur infrequently (<10% of years) in third-order channels in the OCR.

Bed material routed out of one tributary mixes with sediment stored and transported in the receiving channel, as *Jacobson* [1995] documented using long-term (70-year) river cross-section measurements in the Ozark Plateaus. In our calculations the frequency of channel aggradation increases with drainage area in the 25-km^2, fifth-order channel ($s = 0.007$) because of the increasing number of landslide and debris-flow sources upstream and of the increasing cumulative probability of fire (Figure 4b). The increasing number of active upstream sediment sources following fires and storms leads to mixing of sediment waves at confluences and mixing of fluvial sediment with colluvial deposits. As a consequence, periods of channel aggradation (with fluvial bed material only) in the fifth-order channel increase to a maximum of 80 years, and aggraded channel reaches increase in length up to 7 km. The heights of fluvial sediment deposits average 0.6 m and reach a maximum of 1.2 m. Supply-limited conditions in the fifth-order channel

(70% of the time series) are characterized by a bed-material thickness of approximately 0.2 m that arises because of continuously occurring erosion and sediment transport in the watershed, and according to our field observations is expressed as discontinuous gravel sheets over bedrock.

In the field, channels with drainage areas between 15 and 32 km^2 have bed material between 0.1 and 2.0 m thick [*Benda*, 1994], similar to model predictions. The temporal frequency distribution of sediment depths in the fifth-order segment (Figure 5b) is still strongly right skewed, reflecting the fact that although there is an increase in the number of sediment sources downstream, resulting in an increasing opportunity for aggradation after fires (Figure 4) the low probability of fires still results in long periods of sediment supply-limited conditions.

As drainage area increases to 215 km^2 in a sixth-order channel ($s = 0.002$) the sediment supply is more continuous compared to the lower-order channels (Figure 4c). Supply is still much less than transport capacity, however, because the ratio of bed load to total load has declined through attrition of the weak gravel to an average of 4%. The average bed-material thickness and its range are approximately 0.2 m. The high-frequency spikes in the time series of sediment depths (Figure 4c) are the result of either landslides from adjacent bedrock hollows or debris flows from first- and second-order channels that deposit sediment directly into the wide sixth-order channel. Sediment waves passing through the sixth-order segment from upstream are generally longer and of lower amplitude. The predicted average sediment thickness of 0.2 m agrees with our field observations that the lower reaches of the North Fork are floored with only a thin, discontinuous layer of sediment, and bedrock is widely exposed. It is a consequence of the mechanically weak condition of the gravel, and indirectly of the high rates of runoff and the steep channel gradients which ensure that sediment transport rates are high relative to average sediment supply rates, and would presumably be different in other lithologic, hydrologic, and topographic conditions. Large woody debris would also presumably slow the rate of long-term bed material transport rate. Although we have no specific knowledge of the recent history of the North Fork, it is known that such debris was cleared from many of the channels of the area within the past century. However, our laboratory-measured attrition rates and our calculated long-term sediment production rates suggest that attrition strongly limits the amount of gravel that survives transport to sixth-order segments on the Tyee sandstone.

At 215 km^2 the frequency distribution of sediment depths is approximately normal (Figure 5c) because of the integrating effects of the converging, hierarchical drainage network that combines sediment from many different sources in the watershed. Comparison of the three frequency distributions of sediment depths (Figure 5) shows the evolution of the forms of the distribution from an exponential (3 km^2) to a normal distribution at 215 km^2. The evolution of the frequency distributions illustrates how the many point sources of sediment supply in the third-order channels of the network create pulses of sediment or sediment waves that accumulate downstream, eventually creating a Gaussian distribution of sediment depths and sediment supply rates as the additive combined sum of the original exponential distributions [*Benjamin and Cornell*, 1970, p. 252].

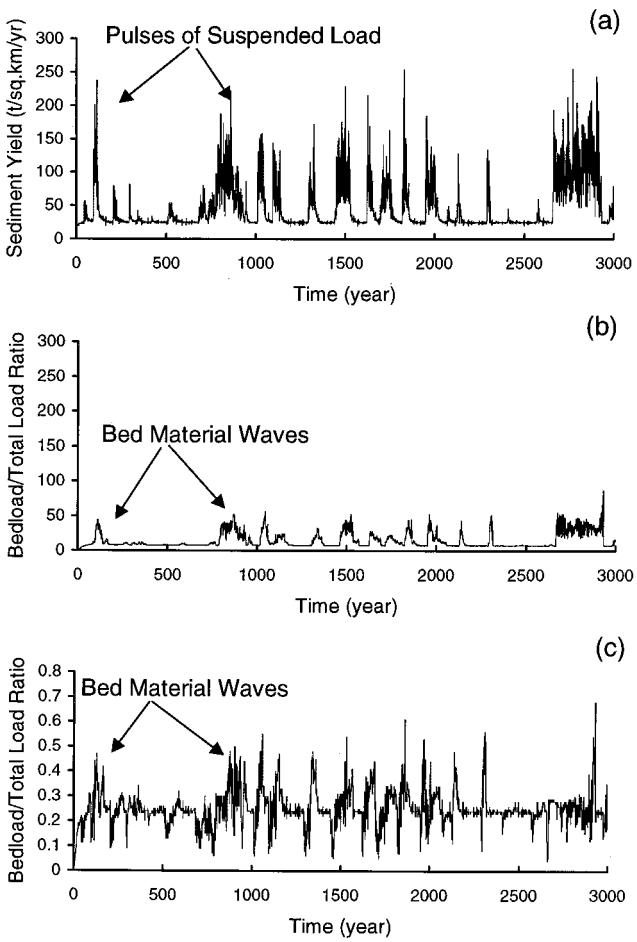

Figure 6. Predicted yields of (a) suspended load and (b) bed load and of (c) bed load/total load ratios in a fifth-order channel segment with a 25-km^2 drainage area.

4.3. Variations in Sediment Transport Rates

Various patterns of sediment transport arise as a consequence of the interactions among the nonuniform and unsteady supply of sediment [*Benda and Dunne*, this issue], the stochastic fluctuation of transport rate (reflecting variations in flow and channel-bed texture and occurrence of woody debris), the hierarchical channel network, and particle abrasion. Although the average sediment yield for the fifth-order channel segment (drainage area = 25 km^2) is approximately 70 t km^{-2} yr^{-1}, the time series is characterized by long periods with yields of approximately 35 t km^{-2} yr^{-1}, punctuated by decades to centuries when bed load and suspended load reach 100–250 t km^{-2} yr^{-1} (Figure 6).

Variations in sediment yields bear complex but identifiable relationships to the ratio of bed load to total load (Figure 6c). For example, during periods of lower sediment yields the ratio of bed load to total load in the fifth-order reach is 0.25, which represents the relative proportions of bed material and suspended load that originate from continuous erosion processes, such as soil creep, bank erosion and fluvial erosion in first- and second-order channels immediately adjacent to the segment and upstream. The ratio also increases upstream during periods of low sediment supply [*Benda*, 1994]. When mass failures deposit colluvium into the fifth-order channel and the stream mines that material, there is an immediate reduction in the

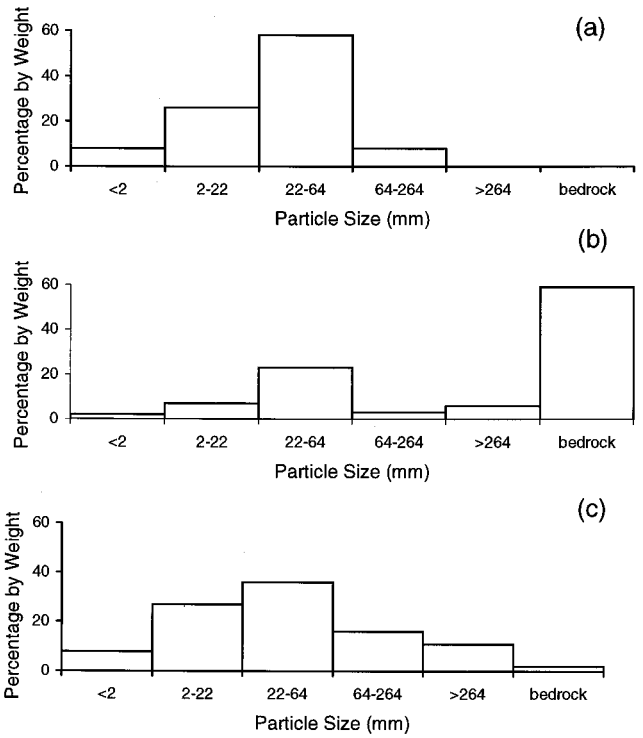

Figure 7. Surface particle-size distributions of channel bed material in three fifth-order channels in the central Oregon Coast Range, each with a different average depth of sediment storage. (a) Harvey Creek is in an aggradational state, (b) Skate Creek is sediment starved, and (c) Franklin Creek is in an intermediate sediment supply state. Textural classes are boulders, >256 mm; cobbles, 64–256 mm; gravel, 2–64 mm; and fines, <2 mm. Data from *Reeves et al*. [1995].

ratio of bed load/total load ratio to 0.1–0.2 because of the immediate flush of suspended load (Figure 6c). That decrease is followed by an increase in the ratio to 0.4–0.6 as bed material moves through the channel segment with only minor suspended load from the originating colluvial deposit. Other fluctuations in the ratio occur because a pulse of suspended load originating from upstream colluvial deposits precedes the syngenetic wave of bed material. The oscillating ratios of bedload to total load indicate the degree to which suspended load and bed load are routed out of the basin out of phase, given our field observation that there is little redeposition of suspended load in the valley floors of the basin [*Benda*, 1995].

In the sixth-order channel segment (215 km^2) the average total sediment yield, comprised almost exclusively of suspended load (average ratio of bed load to total load is 0.04), is approximately 70 t km^{-2} yr^{-1}, and the range of variation in sediment yields is between 50 and 200 t km^{-2} yr^{-1}. The frequency of variation in sediment yields in the sixth-order channel increases compared to the fifth-order channel, similar to the increasing fluctuations in sediment thickness shown in Figure 4c, because of mixing of many sediment sources from upstream, but the relative range of variation declines from about 7 times the average in the fifth-order channel to about 4 times the average in the sixth-order channel.

4.4. Influence of Variable Channel Sediment Storage on Channel Morphology

Sediment waves are often associated with a rise of the channel bed, shallowing of pools, and development of a plane-bed geometry and low, poorly defined banks [*Griffiths*, 1979; *Roberts and Church*, 1986; *Madej and Ozaki*, 1996]. Relatively fine particles persist in a reach through which they were formerly transported quickly, and they tend to fill pools. To determine how sediment waves or periods of channel aggradation and degradation influence channel morphology in the sandstone basins of the central OCR, we selected reaches of three streams with similar drainage areas and gradients. Although the history of fire and mass wasting in each is not well known, there are large differences in the average depths of sediment stored in them. We used them to examine the association between sediment storage and channel-bed texture and pool depth. *Reeves et al*. [1995] measured sediment depths, pool depths, and bed-surface grain sizes (Figures 7 and 8) in each of two consecutive years. Field-measured average bed-material thickness for each reach is shown by initials on Figure 5b, to indicate the sediment supply condition relative to predicted frequency distributions of sediment depths for a similarly sized channel segment. The sediment thicknesses were measured over long reaches and did not reflect merely storage behind log jams.

Harvey Creek (drainage area = 18 km^2; $s = 0.0085$) has an average sediment thickness of 1.8 m but relatively little large woody debris except for burned, buried logs and therefore is analogous to reaches in an aggradational or wave state ("HR" in Figure 5b). The channel is dominated by gravel and pebbles which inundate boulders (Figure 7a), and by pools that average

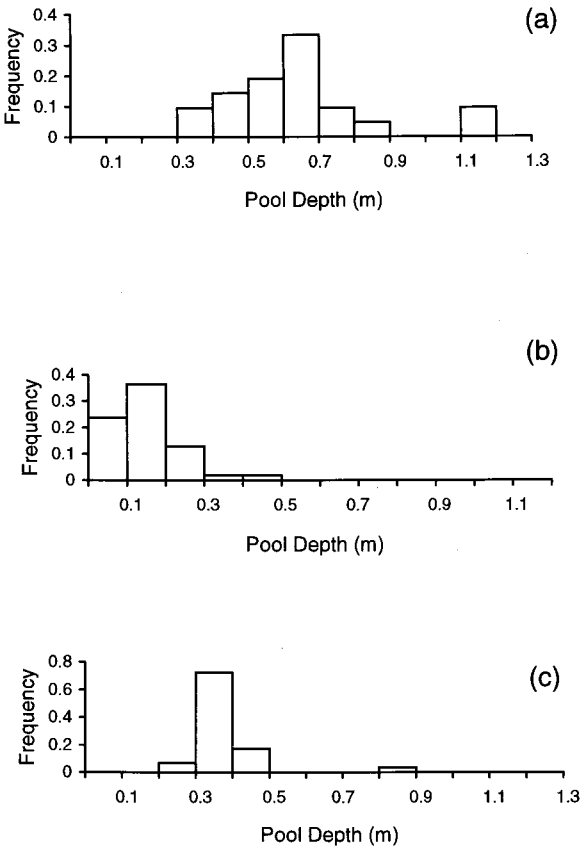

Figure 8. Distribution of pool depths in three fifth-order channels referred to in Figures 5b and 7. (a) Harvey Creek is in an aggradational state, (b) Skate Creek is sediment impoverished, and (c) Franklin Creek is in an intermediate sediment supply state. Unpublished data from G. H. Reeves, U.S. Forest Service, Corvallis, Oregon, 1994, 1995.

0.5 m in depth (Figure 8), though most of the pools are dry during the summer low flow. Skate Creek (area = 14 km^2; s = 0.0094) has an average bed-material thickness of <0.1 m ("SK" in Figure 5b) with more than 60% of the channel floored by bedrock (Figure 7) and thus appears to be in a sediment-supply-limited or nonwave state. Channel morphology in Skate Creek is characterized by bedrock and boulder substrate with small patches of finer sediment (Figure 7b), pools that average 0.15 m in depth (Figure 8b), and a larger number of logs recruited from the older streamside forests. The third basin, Franklin Creek (area = 15 km^2; s = 0.0093) has average sediment depths of 0.5 m ("FR" in Figure 5b). The bed-material texture in Franklin Creek is more heterogeneous (Figure 7c), while pool depths averaging 0.3 m (Figure 8c) and abundance of woody debris are intermediate between those of Harvey and Skate Creeks. Thus despite approximate equality of drainage area and gradient, these channel reaches had significantly different channel morphologies and bed textures associated with differences, presumably transient, in the average depth of sediment stored in them. Thus our approach provides a means of analyzing the most probable and range of transient conditions of sediment supply and transport that *Montgomery and Buffington* [1997] call upon to explain their classes of channel morphology.

Although the reaches used to determine the effects of sediment storage on channel morphology had drainage areas of 14–18 km^2 and gradients of approximately 0.009, the association between morphology, bed texture, and the volume of bed material in storage should also apply to other channels with different drainage areas in the OCR. For example, our field observations in third-order channels indicate similar associations between bed texture, morphology, and sediment storage, although according to our model the various associations should occur with different frequencies and magnitudes. Also, both model simulations and field observations indicate that channels with drainage areas greater than approximately 100 km^2 in this region are predominantly bed load supply limited, and hence little change in channel morphology would be expected there as a result of perturbations in sediment supply.

5. Probabilistic Approach to Basin-Wide Sedimentation and Channel Morphology

Field evidence in the OCR indicates that large fires and rainstorms lead to concentrated landsliding and debris flows and thus to punctuated sediment supply to channels [*Benda and Dunne*, this issue, Figure 3]. Model simulations of these interactions on large aggregates of hillslopes suggest the structure of the spatial and temporal patterns of erosion and sediment supply to channels [*Benda and Dunne*, this issue, Figure 12].

The nonuniform and unsteady characteristics of sediment routing and storage in river channels that are predicted to result from the punctuated supply (Figures 4–6) argue for a probabilistic approach to certain aspects of fluvial geomorphology in the OCR. Such an approach suggests a greater range of conditions and behavior, including the importance of transition between states, than that which is likely to be captured by measurements obtained over short periods in a few locations. Yet basin-scale summaries of sediment transport or channel morphology currently take no account of temporal variation longer than a single flood.

In such dynamic environments, even those not dominated by debris-flow sedimentation, periods of channel aggradation and degradation, or the frequency and magnitude of sediment routing and storage and associated channel morphology, may be described in terms of probabilities. For example, one can define the probability of a fluvial bed-material wave state after choosing a definition of minimum sediment thickness for a wave on the basis of some field observation of channel behavior. On the basis of field observations in the OCR that 0.3 m of bed material over bedrock is sufficient to transform a bedrock channel into one with some alluvial characteristics, such as deformable pools and riffles, we define a sediment-wave state as an increase in bed elevation of greater than 0.3 m above the background condition caused by the passage of fluvially transported bed material. (A separate definition could be used to isolate waves of colluvium.) The probability of encountering an aggraded channel or a sediment-wave state in any year was then computed by multiplying the modeled frequency of aggradation by the average duration of aggradation in each of the 370 channel segments in the North Fork of the Smith River. The probability of aggradation with bed material in any year is least in the smallest drainage areas (0.05 at drainage areas less than 10 km^2), because of the low frequency of landslides and debris flows from the limited number of sediment source areas (Figure 9a). These channels are supply-limited environments (bedrock and boulder-floored), punctuated by episodic influxes of colluvium from debris flows and landslides which lead to brief periods of colluvium-bed [sensu *Montgomery and Buffington*, 1997, p. 602] or gravel-bed morphology. The probability of channel aggradation increases to 0.35 as drainage area increases to approximately 50 km^2, because the hierarchical channel network integrates the effects of the increased number of upstream landslide and debris-flow source areas as well as of fires. The probability of an aggraded channel (i.e., of wave-like storage) decreases to less than 0.15 as drainage area increases to 215 km^2 in the North Fork, because particle attrition lowers the ratio of bed load to total load and because channel widening reduces the thickness of bed material. A very low probability (<0.05) of channel aggradation occurs in a narrow canyon that has small, local contributing areas and no major tributaries (Figure 9a). In other landscapes with higher erosion rates or gravel that is less vulnerable to abrasion, the higher-order channels may contain thicker deposits of gravel, especially where the river profiles are more concave than those in our study area. In addition, local decreases in channel slope and increases in valley-floor width, caused by earth flow [*Swanston*, 1981], debris-flow deposits [*Benda*, 1988], or geologic structure may locally increase the probability of aggradation and the subsequent development of terraces associated with wave passage. The magnitude of wave-like bed load transport, as a proportion of the total bed load yield, follows the same pattern as the wave-state probability, for similar reasons (Figure 9b). However, the majority of bed load transport occurs at more or less uniform rates in the study basin because of chronic erosion processes such as soil creep, bank erosion of fans and terraces, and fluvial erosion in first- and second-order channels.

The high-order network of the North Fork Smith River can be classified with respect to the long-term average frequency and magnitude of changes in sediment storage and transport (Figure 10), although the simulations also define abrupt local changes that take place at and immediately downstream of tributary junctions [*Benda*, 1994, Figure 8-18]. This generalized map of the space-time structure of sediment storage and routing pertains to the central OCR. We expect it to change in different landscapes with other climates, fire characteristics,

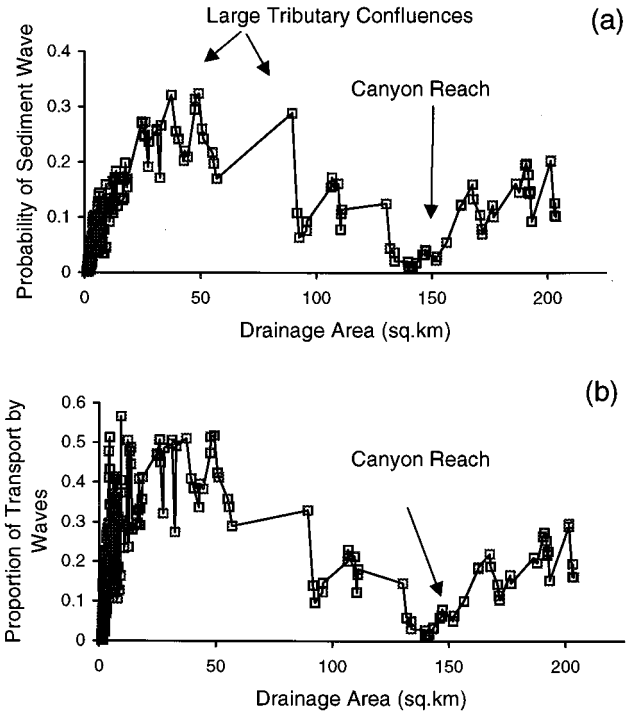

Figure 9. (a) Probability of a wave state, defined as channel aggradation of 0.3 m or greater above the continuous background sediment supply condition as a function of drainage area for all 370 channel segments. (b) Proportion of total bed load transported in sediment waves for all 370 segments over 3000 years of the simulation.

channel networks, and rock types. The model that we have proposed here can be used to examine systematically the changes in the space-time structure of sedimentation to be expected from such environmental variables.

When the general stochastic principle that we are articulating is applied to mountain channel networks, a pattern such as Figure 10 can also be mapped onto the spatial classification of mountain channel morphology proposed by *Montgomery and Buffington* [1997]. It adds a classification of channels in terms of the magnitude and frequency of sediment storage change. Although our model deals explicitly only with a few morphological aspects of channels, such as whether they are deeply or thinly buried or not buried with sediment, it also suggests that the morphologies that Montgomery and Buffington recognize are the most probable states of the channel in particular reaches: colluvium-rich, bedrock- and boulder-controlled channels are more likely to be encountered during a survey of low-order channels, and the probability of continuous alluvial cover increases downstream. Our model also provides a process-based explanation for the spatially varying ratio of sediment supply to transport capacity with which *Montgomery and Buffington* [1997, Figures 10, 11] explain the systematic change of channel morphology with drainage area and gradient. Our calculations also illustrate the likelihood, spatial patterns, and causes of transient sediment storage and of morphological responses such as bed-elevation changes, and alternation of bedrock- and boulder-controlled channels with sediment-rich channels. Inclusion of abrasion in our model also allows us to add the prediction that at large drainage areas and low gradients in some lithologies one might expect thin, patchy alluvium or bedrock-floored channels, of the type occurring in the field area, rather than the pool-riffle morphology that is more widespread [*Montgomery and Buffington*, 1997].

6. Summary

Model predictions suggest that waves of sediment storage and transport with characteristic length and height scales are a fundamental characteristic of sediment transport systems in basins where portions of the sediment influx to channels are nonuniform and unsteady. This testable, theoretical finding based on our simulation in the OCR is consistent with numerous field measurements and observations of transient aggradation, commonly referred to as sediment waves, linked to concentrated erosion worldwide. We have proposed a generalizable scheme for systematically analyzing how such pulses of sediment transport and storage might arise, migrate, and interact because of the interplay between hillslope supply processes, fluctuating sediment transport rates, channel network characteristics, particle attrition, and the more fundamental geologic, climatic, and topographic factors that control them. Testing of the proposal requires regional or basin-wide sampling and dating of sediment deposits, rather than confinement of sediment transport studies to reach-length process mechanics. The approach also allows one to examine the influence of basin scale on the spectra of sediment transport and storage and associated textural and morphologic change. Quantifying the influence of basin scale on these spectra can lead to classifying reaches of river networks in terms of the expectable frequency and magnitude of sediment flux and storage, and variations in channel morphology.

The combined stochastic models of sediment supply [*Benda and Dunne*, this issue] and routing could also be used to examine the general nature of changes in sedimentation to be expected from altering one or more of the controlling variables, such as the probability distribution of sediment transport rates or fire frequency. Geographical variations in the controlling variables between regions can also be rationalized in the same manner. Such analyses would require careful transfer of empirical information (rainfall probabilities, tree-root strengths, sediment transport probability distributions, etc.) between times and regions as well as the collection of some new field information. Both techniques are standard in hydrology and geomorphology, however. A bigger difficulty is that of judging the linkages between, for example, rainstorm probabilities that affect hillslope stability and sediment supply and the probability distribution of sediment transport rates in a region. That is a secondary topic for further research, however, and in the meantime significant insights about the space-time structure of sediment transport and storage can be gained through incorporating the simplest hypotheses about controlling variables in a scheme such as we propose here.

The specific model predictions of frequency and magnitude of sediment transport and storage in any basin are approximate, given the uncertainties of process formulation, the inherent variability and unpredictability (except in a statistical sense) of the climatic and geomorphic parameters in our model, and the absence from the model of other processes such as sediment storage in terraces and behind log jams. However, the general model predictions indicate how unsteady and nonuniform supply of sediment can arise in a basin over time. The systematic predictions of how spatial scale (drainage area), channel network topology, particle abrasion, and climate influence the frequency and magnitude of wave-like sediment

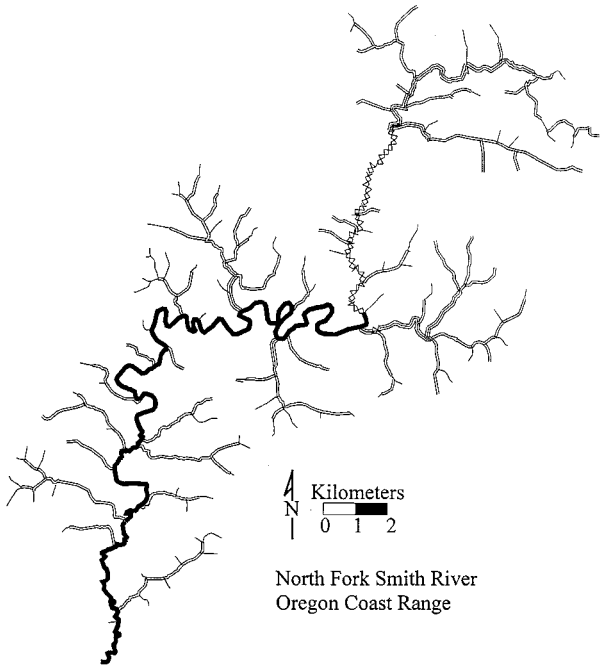

Frequency Characteristics of Sediment Storage in the Channel Network

Map Symbol	Drainage Area (km^2)	Probability (of channel aggradation)	Amplitude (of aggradation) Ave/Max (m)	Duration (of aggradation) Ave/Max (yrs)	Length (of channel affected) Ave/Max (km)	Bed Substrate (most frequent)
	0.5 - 1.0	< 0.05	0.6 / 2.5	2 / 20	0.2 / 2	Bedrock/Boulders
	1 - 10	0.20	0.5 / 2.5	5 / 80	0.5 / 10	Gravel/Bedrock
	10 - 35	0.25	0.5 / 2.0	5 / 90	1 / 12	Gravel/Bedrock
	35 - 70	0.20	0.4 / 1.5	10 / 120	1 / 8	Bedrock/Boulders
	70 - 200	0.10	0.3 / 0.5	1 / 80	0.2 / 4	Bedrock/Boulders

Figure 10. A classification of the third- and higher-order channel network according to the characteristics of wave-like sediment transport. Within the reaches demarcated by uniform line symbols, the probabilities and other characteristics change uniformly with abrupt changes at tributary junctions.

transport should apply to other mountain environments, even to those in which mass wasting is from larger and more continuously active features, such as earth flows [*Swanston*, 1981], or where the episodic effects are due to influences such as earthquakes [*Pearce and Watson*, 1986].

Acknowledgments. This work was supported by Cooperative Agreements PNW 93-0422 and 94-0574 with the U.S. Forest Service Pacific Northwest Forest and Range Experiment Station, Portland. We are grateful to R. L. Bras, V. K. Gupta, and I. Rodriguez-Iturbe for stimulating our original interest in stochastic forcing of geomorphic processes at a workshop on scale effects in hydrology. Daniel Miller assisted us at many stages of the work with insightful suggestions and with computing. J. Gabrielson wrote the computer program. We also appreciate improvements to the manuscript suggested by T. E. Lisle, D. J. Miller, D. R. Montgomery, C. Paola, and L. M. Reid.

References

Bagnold, R. A., Experiments on a gravity-free dispersion of large solid spheres in a Newtonian fluid under shear, *Proc. R. Soc. London A*, *225*, 49–63, 1954.

Bagnold, R. A., The nature of saltation and of 'bedload' transport in water, *Proc. R. Soc. London A*, *332*, 473–504, 1973.

Barnes, H. H., Roughness characteristics of natural channels, *U.S. Geol. Surv. Water Supply Pap. 1849*, 1967.

Benda, L., Debris flows in the Oregon Coast Range, M.S. thesis, 127 pp., Univ. of Wash., Seattle, 1988.

Benda, L., The influence of debris flows on channels and valley floors of the Oregon Coast Range, U.S.A., *Earth Surf. Processes Landforms*, *15*, 457–466, 1990.

Benda, L., Stochastic geomorphology in a humid mountain landscape, Ph.D. thesis, 353 pp., Univ. of Wash., Seattle, 1994.

Benda, L., Stochastic geomorphology—implications for monitoring and interpreting erosion and sediment yields in mountain drainage basins, in *Proceedings, Effects of Scale on Interpretation and Management of Sediment and Water Quality*, *IAHS Publ. 226*, 47–54, 1995.

Benda, L., and T. Dunne, Sediment routing by debris flow, *Proceedings, Symposium on Erosion and Sedimentation in the Pacific Rim*, *IAHS Publ. 165*, 213–223, 1987.

Benda, L., and T. Dunne, Stochastic forcing of sediment supply to channel networks from landsliding and debris flow, *Water Resour. Res.*, this issue.

Benjamin, J. R., and C. A. Cornell, *Probability, Statistics, and Decision Making for Civil Engineers*, 684 pp., McGraw-Hill, New York, 1970.

Beschta, R. L., Long-term patterns of sediment production following road construction and logging in the Oregon Coast Range, *Water Resour. Res.*, *14*, 1014–1016, 1978.

Beschta, R. L., Patterns of sediment and organic-matter transport in Oregon Coast Range streams, in *Proceedings, Symposium on Erosion*

and Sediment Transport in Pacific Rim Steeplands, *IAHS Publ. 132*, 179–188, 1981.

Beschta, R. L., River channel response to accelerated mass soil erosion, in *Proceedings, Symposium on Effects of Forest Land Use on Erosion and Slope Stability*, pp. 155–164, East-West Cent., Univ. of Hawaii, Honolulu, 1984.

Bodhaine, G. L., and D. M. Thomas, Magnitude and frequency of floods in the U.S., 12, Pacific Slope basins in Washington and Upper Columbia River basin, *U.S. Geol. Surv. Water Supply Pap. 1687*, 1964.

Brown, G. W., and J. T. Krygier, Clear-cut logging and sediment production in the Oregon Coast Range, *Water Resour. Res*., *7*, 1189–1198, 1971.

Church, M., and M. A. Hassan, Size and distance of travel of unconstrained clasts on a streambed, *Water Resour. Res*., *28*, 299–303, 1992.

Collins, B. D., and T. Dunne, Gravel transport, gravel harvesting and channel-bed degradation in rivers draining the southern Olympic Mountains, Washington, U.S.A., *Environ. Geol. Water Sci*., *13*, 213–224, 1989.

Collins, B. D., T. J. Beechie, L. E. Benda, P. M. Kennard, C. N. Veldhuisen, V. S. Anderson, and D. Berg, Watershed assessment and salmonid habitat restoration strategy for Deer Creek, North Cascades of Washington, 231 pp., 10,000 Years Inst., Seattle, Wash., 1994.

Dietrich, W. E., and T. Dunne, Sediment budget for a small catchment in mountainous terrain, *Z. Geomorph. Suppl*., *29*, 191–206, 1978.

Dietrich, W. E., T. Dunne, N. F. Humphrey, and L. M. Reid, Construction of sediment budgets for drainage basins, in *Sediment Budgets and Routing in Forested Drainage Basins*, *Gen. Tech. Rep. PNW Pac. Northwest For. Range Exp. Stn. PNW-141*, pp. 5–23, 1982.

Dietrich, W. E., J. W. Kirchner, H. Ikeda, and F. Iseya, Sediment supply and the development of the coarse surface layer in gravel bedded rivers, *Nature*, *340*, 215–217, 1989.

Everest, F. H., and W. R. Meehan, Some effects of debris torrents on habitat of anadromous salmonids, *Tech. Bull. 353*, pp. 23–30, Natl. Counc. of the Pap. Ind. for Air and Stream Impr., New York, 1981.

Gell-Man, M., *The Quark and the Jaguar: Adventures in the Simple and the Complex*, 329 pp., W. H. Freeman Co., New York, 1994.

Gilbert, G. K., Hydraulic-mining debris in the Sierra Nevada, *U.S. Geol. Surv. Prof. Pap. 105*, 154 pp., 1917.

Griffiths, G. A., Recent sedimentation history of the Waimakariri River, New Zealand, *J. Hydrol. N. Z*., *18*, 6–28, 1979.

Hassan, M. A., and M. Church, Virtual rate and mean distance of travel of individual clasts in gravel-bed channels, *Earth Surf. Processes Landforms*, *17*, 617–627, 1992.

Horton, R. E., Hydrophysical approach to the morphology of hillslopes and drainage basins, *Geol. Soc. Am. Bull*., *56*, 275–370, 1945.

Jacobson, R. B., Spatial controls on patterns of land-use-induced stream disturbance at the drainage-basin scale—an example from gravel-bed streams of the Ozark Plateaus, *Eos Trans. AGU*, *76*(17), Spring Meet. Suppl., 151, 1995.

Kelsey, H. M., R. Lamberson, and M. A. Madej, Stochastic model for the long-term transport of stored sediment in a river channel, *Water Resour. Res*., *23*, 1739–1750, 1987.

Klock, G. O., and J. D. Helvey, Debris flows following wildfire in north central Washington, in *Proceedings of Third Federal Interagency Sedimentation Conference*, pp. 1-91–1-98, Water Resour. Counc. Sediment. Comm., Denver, Colo., 1976.

Leopold, L. B., and W. W. Emmett, Bedload measurements, East Fork River, Wyoming, *Proc. Natl. Acad. Sci. U. S. A*., *73*, 1000–1004, 1976.

Lisle, T. E., Effects of aggradation and degradation on riffle-pool morphology in natural gravel channels, northwestern California, *Water Resour. Res*., *18*, 1643–1651, 1982.

Madej, M. A., Sediment transport and channel changes in an aggrading stream in the Puget Lowland, Washington, in *Sediment Budgets and Routing in Forested Drainage Basins*, *Gen. Tech. Rep. PNW Pac. Northwest For. Range Exp. Stn*., *PNW-141*, pp. 97–108, 1982.

Madej, M. A., and V. Ozaki, Channel response to sediment wave propagation and movement, Redwood Creek, California, USA, *Earth Surf. Processes Landforms*, *21*, 911–927, 1996.

Meade, R. H., Wavelike movement of bedload sediment, East Fork River, Wyoming, *Environ. Geol. Water Sci*., *7*, 215–225, 1985.

Megahan, W. F., Channel sediment storage behind obstructions in forested drainage basins draining the granitic bedrock of the Idaho batholith, in *Sediment Budgets and Routing in Forested Drainage Basins*, *Gen. Tech. Rep. PNW Pac. Northwest For. Range Exp. Stn. PNW-141*, pp. 114–121, 1982.

Milhous, R. T., Sediment transport in a gravel-bottomed stream, Ph.D. thesis, 232 pp., Oreg. State Univ., Corvallis, 1973.

Montgomery, D. R., and J. M. Buffington, Channel-reach morphology in mountain drainage basins, *Geol. Soc. Am. Bull*., *109*, 596–611, 1997.

Mosley, M. P., Bed material transport in the Tamaki River near Dannevirke, North Island, New Zealand, *N. Z. J. Sci*., *21*, 619–626, 1978.

Nakamura, F., Chronological study on the torrential channel bed by the age distribution of deposits, *Res. Bull. Coll. Exp. For. Hokkaido Univ*., *43*, 1–26, 1986.

Nicholas, A. P., P. J. Ashworth, M. J. Kirkby, M. G. Macklin, and T. Murray, Sediment slugs: Large-scale fluctuations in fluvial sediment transport rates and storage volumes, *Prog. Phys. Geogr*., *19*, 500–519, 1995.

O'Connor, M. D., Bedload transport processes in steep tributary streams, Olympic Peninsula, Washington, U.S.A., *Adv. Hydro-Sci. Eng*., *1*, 243–251, 1993.

Ouchi, S., Tombi landslide and its impact on the Joganji River, Japan, in *Proceedings, Symposium on Erosion and Sedimentation in the Pacific Rim*, *IAHS Publ. 165*, 135–136, 1987.

Pain, C. F., and P. L. Hosking, The movement of sediment in a channel in relation to magnitude and frequency concepts: A New Zealand example, *Earth Sci. J*., *4*, 17–23, 1970.

Pearce, A. J., Geomorphic effectiveness of erosion and sedimentation events, *J. Water Resour*., *5*, 551–568, 1986.

Pearce, A. J., and A. J. Watson, Effects of earthquake-induced landslides on sediment budget and transport over a 50-year period, *Geology*, *14*, 52–55, 1986.

Perkins, S. J., Landslide deposits in low-order streams—their erosion rates and effects on channel morphology, in *Proceedings, Symposium on Headwater Hydrology*, *TPS-89-1*, pp. 173–182, Am. Water Resour. Assoc., Bethesda, Md., 1989.

Pickup, G., R. J. Higgins, and I. Grant, Modelling sediment transport as a moving wave—the transfer and deposition of mining waste, *J. Hydrol*., *60*, 281–301, 1983.

Reeves, G. H., L. E. Benda, K. M. Burnett, P. A. Bisson, and J. R. Sedell, A disturbance-based ecosystem approach to maintaining and restoring freshwater habitats of evolutionarily significant units of anadromous salmonids in the Pacific Northwest, in *Symposium on Evolution and the Aquatic System: Defining Unique Units in Population Conservation*, vol. 17, pp. 334–349, Am. Fish. Soc., Bethesda, Md., 1995.

Reneau, S. L., and W. E. Dietrich, Erosion rates in the southern Oregon Coast Range: evidence for an equilibrium between hillslope erosion and sediment yield, *Earth Surf. Processes Landforms*, *16*, 307–322, 1991.

Roberts, R. G., and M. Church, The sediment budget in severely disturbed watersheds, Queen Charlotte Ranges, British Columbia, *Can. J. For. Res*., *16*, 1092–1106, 1986.

Swanson, F. J., Fire and geomorphic processes, in *Fire Regimes and Ecosystem Properties*, *Gen. Tech. Rep. WO U.S. For. Serv. WO-26*, pp. 401–420, 1981.

Swanson, F. J., and G. W. Lienkaemper, Physical consequences of large organic debris in Pacific Northwest streams, *Gen. Tech. Rep. PNW Pac. Northwest For. Range Exp. Stn. PNW-69*, 12 pp., 1978.

Swanston, D. N., Creep and earthflow erosion from undisturbed and management impacted slopes in the Coast and Cascade Ranges of the Pacific Northwest, U.S.A., in *Proceedings, Symposium on Erosion and Sediment Transport in Pacific Rim Steeplands*, *IAHS Publ. 132*, 76–95, 1981.

VanSickle, J., and R. L. Beschta, Supply-based models of suspended sediment transport in streams, *Water Resour. Res*., *19*, 768–778, 1983.

Wohl, E. E., and P. P. Pearthree, Debris flows as geomorphic agents in the Huachuca Mountains of southeastern Arizona, *Geomorphology*, *4*, 273–292, 1991.

Wolman, M. G., and J. P. Miller, Magnitude and frequency of forces in geomorphic processes, *J. Geol*., *68*, 54–74, 1960.

L. Benda, Earth Systems Institute, 1314 NE 43rd St., Suite 207, Seattle, WA 98105-5832. (e-mail: leebenda@aol.com)

T. Dunne, School of Environmental Science and Management, University of California, 4670 Physical Sciences North, Santa Barbara, CA 93106-5131. (e-mail: tdunne@esm.ucsb.edu)

(Received October 23, 1995; revised August 18, 1997;
accepted August 22, 1997.)